

# **SOIL AND ROCK AMERICA 2003**

**12<sup>th</sup> Panamerican Conference on Soil Mechanics  
and Geotechnical Engineering**

**12<sup>o</sup> Conferencia Panamericana de Mecánica de Suelos  
e Ingeniería Geotécnica**

**39<sup>th</sup> U.S. Rock Mechanics Symposium**

June 22 - 26, 2003  
Cambridge, Massachusetts, USA

**PROCEEDINGS VOLUMES 1 AND 2**

*Edited by:*

**Patricia J. Culligan  
Herbert H. Einstein  
Andrew J. Whittle**

*Massachusetts Institute of Technology*

**VGE**  
Verlag Glückauf Essen

VERLAG GLÜCKAUF GMBH · ESSEN (GERMANY) 2003

# Analysis of a Void Redistribution Mechanism in Liquefied Soil

## Análisis de un Mecanismo de Redistribución de Vacíos en Suelo Licuado

Malvick, E. J., Kulasingam, R., Boulanger, R. W., and Kutter, B. L.  
*University of California, Davis*

### Abstract

*An analysis of a void redistribution mechanism in liquefied soil is presented for a layered infinite slope. Excess pore water pressure generated by earthquake loading produces upward seepage. Pore water expelled from the lower contracting zones of the liquefied layer can become trapped at an interface with an overlying lower-permeability layer. This trapped water can cause local loosening (void ratio increase) near the interface and potentially form a water film. The potential for this void redistribution to cause instability is shown to strongly depend on the sand's relative density, the slope angle, and the sand layer thickness. The initial thickness of the dilating (loosening) zone at the top of the sand layer was shown to be much greater than the eventual thickness of any shear localizations (e.g. 10's of grain diameters). Accounting for the initial thickness of this dilating zone avoids an overly conservative assessment of the conditions that lead to instability.*

### Resumen

*Se presenta un análisis de un mecanismo de redistribución de vacíos en suelo licuado para un talud infinito estratificado. Las presiones de poros de exceso generadas por las cargas inducidas por terremotos produce filtración ascendente. El agua de los poros expulsada de las zonas de baja contracción en la capa licuada puede atraparse en el interfaz con una capa sobrepuesta de baja permeabilidad. Esta agua atrapada puede causar que el material se suelte localmente (aumento de la relación de vacíos) cerca del interfaz y potencialmente forme una película de agua. Se demuestra que el potencial para que esta redistribución de vacíos cause inestabilidad depende fuertemente de la densidad relativa de la arena, del ángulo del talud y del espesor de la capa de la arena. Se demostró que el espesor inicial de la zona de dilatación (zona suelta) en el tope de la capa de arena es mucho mayor que el espesor de cualquier zona de corte eventual localizada (equivalente a decenas de diámetros de granos). El tener en cuenta el espesor inicial de esta zona de dilatación evita una estimación excesivamente conservadora de las condiciones que conducen a la inestabilidad.*

## 1 INTRODUCTION

Void redistribution during earthquake-induced liquefaction can cause localized loosening (dilation) and concentrated shear deformations that contribute to overall deformations or instability of slopes or embankments (Whitman 1985, NRC 1985). The key consequence of void redistribution is that the liquefied soil's shear strength and stress-strain response are not solely dependent on the pre-earthquake material properties and state (e.g.,  $D_r$  and  $\sigma'$ ), but rather can also reflect the response of the entire system. The effects of void redistribution are not well

understood, universally accepted, nor explicitly accounted for in engineering practice.

The formation of water films, which is an extreme case of void redistribution, has been observed or inferred under level ground conditions in a number of physical model studies (e.g., Liu & Qiao 1984, Dobry & Liu 1992, Fiegel & Kutter 1994) and simple cylindrical column tests (e.g., Kokusho 1999). The experimental data and associated analyses illustrate the importance of stratigraphy (layer thickness, sequence), permeability contrasts, and relative density ( $D_r$ ) on the resulting water film thickness.

For sloping ground conditions, Kokusho (1999) reported the formation of water films beneath silt

arcs embedded in slopes of very loose sands in 1-g shake table tests. Kulasingam (2003) and Malvick et al. (2002) reported the formation of localized shear zones, without evidence of water film formation, beneath silt arcs in simple slopes of sand at  $D_r$  of 20 to 50% in centrifuge tests.

The centrifuge tests by Malvick et al. (2002) showed that the formation of localized shear due to void redistribution depended on the sand's  $D_r$ , the thickness of the sand layers, the shaking duration, and the shaking history. Above a certain  $D_r$ , certain shaking motions did not cause localizations despite having produced the same levels of excess pore water pressures observed in looser models. Note that excess pore water pressure ratios ( $r_u$ ) have limiting values, which are less than 100% for sloping ground conditions and are generally associated with shear strains greater than about 3% (Boulanger & Seed 1995). In this paper "liquefaction" refers to the generation of these limiting  $r_u$  values.

The stress-strain response of liquefied sand to the inflow of pore water from adjoining zones under sloping ground conditions was illustrated in laboratory tests by Boulanger and Truman (1996), Tokimatsu et al. (2001), and Vaid and Eliadorani (1998). A net inflow of pore water to a sand element that carries a static shear stress (which is insufficient to cause flow if purely undrained) and already at its limiting  $r_u$ , produces small changes in excess pore pressure while being accommodated by dilation (loosening) of the sand towards critical state.

The thickness of a dilating (loosening) shear zone can be an important factor affecting the potential for void redistribution induced instability of a slope. Consider the infinite slope example in Figure 1. If the overlying low-permeability layer precludes any significant pore water drainage in the time of interest, then the volume of water expelled from the contracting (densifying) lower portion of the liquefied sand layer will all accumulate at the top of the sand layer. If the dilating shear zone is only about 10 to 20 times the median grain diameter ( $D_{50}$ ), then it takes very little inflow to drive the shear zone to critical state and instability. In that scenario, the triggering of high excess pore pressure ratios in relatively thin layers of medium-dense sand could lead to instability due to void redistribution.

However, the thickness of the dilating zone was shown by Boulanger and Truman (1996) and Boulanger (1999) to be much greater than 10's of  $D_{50}$  based on an infinite slope analyses that considered the stress-strain response of the liquefied sand to inflow of pore water from

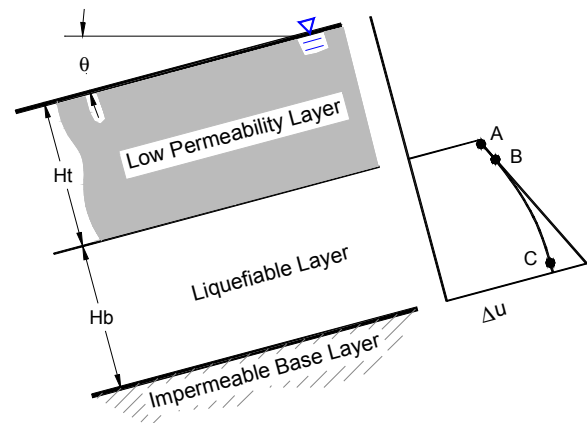


Figure 1: Potential mechanism for void redistribution within a layered infinite slope.

adjoining zones.

This paper presents an analysis of void redistribution in a confined liquefied sand layer in an infinite slope. The analysis method expands upon the method in Boulanger and Truman (1996) to illustrate the influence of relative density, layer thickness ( $H_b$ ), and slope angle ( $\theta$ ) on the potential for void redistribution. First, the general features of the void redistribution mechanism and related soil behavior are described. Then a detailed example is presented, followed by a parametric study. The analyses results demonstrate how the thickness of the dilating (loosening) zone depends on  $D_r$  and  $\theta$ , and identifies the combinations of  $\theta$ ,  $H_b$ , and  $D_r$  that can theoretically lead to instability.

The above analyses are followed by a discussion of several complicating factors that limit our ability to reliably predict the occurrence and consequences of void redistribution in the field. Nonetheless, it is believed that the analyses serve to identify key behavioral aspects that are important for developing a understanding of void redistribution mechanisms.

## 2 AN IDEALIZED INFINITE SLOPE

First, the general behavior is discussed for the idealized infinite slope shown in Figure 1. A liquefiable sand layer of thickness  $H_b$  is underlain by an impermeable base and overlain by a low-permeability layer. The water table is at the ground surface with steady seepage parallel to the slope.

Earthquake shaking generates excess pore pressures ( $\Delta u$ ) within the sand layer that result in an upward hydraulic gradient,  $i$ , as illustrated by the  $\Delta u$  isochrone in Figure 1. Points A, B, and C experience three different behaviors due to liquefaction and void redistribution. Point C has a

larger  $i$  exiting it than entering it, and thus the soil contracts (densifies). Point B has the same  $i$  entering and exiting, and thus the soil remains at constant volume. Point A dilates (loosens) as a result of a net inflow of water due to the low-permeability confining layer restricting outflow at that location. The overlying layer can restrict the sand layer to be globally undrained during the time of interest if it is thick enough and of sufficiently low permeability.

Pore water flow within the sand layer can be described (Kulasingam 2003) in part by a time factor,  $T_{s,b} = (k_b \cdot t_s) / (m_{v,b} \cdot \gamma_w \cdot H_b^2)$ , where  $k_b$  = hydraulic conductivity of bottom layer,  $m_{v,b}$  = coefficient of volume compressibility of bottom layer,  $H_b$  = thickness of bottom layer, and  $t_s$  = duration of shaking. For  $T$  less than about 0.1, the majority of the net inflow to Point A occurs after shaking for most situations. For simplicity, the analysis presented herein assumes that such a condition applies and that the sand can be considered essentially undrained during shaking with all pore water movement occurring after shaking. In addition, it is assumed that the duration and level of shaking is just sufficient bring the sand layer to limiting  $r_u$  (i.e., a Factor of Safety of 1 against triggering). These assumptions do not alter the void redistribution mechanism but greatly simplify the analysis.

Figure 2 is a schematic of potential stress paths for points A and C under cyclic loading and void redistribution. The sand is assumed to be sufficiently dense that its undrained steady state shear strength ( $S_{us}$ ) is greater than the static shear stresses imposed on it (The alternative case is trivial as it leads to instability without void redistribution). Undrained cyclic loading of sand with an initial static shear stress causes the excess pore pressure ( $\Delta u$ ) to increase until it reaches a limiting level (or limiting residual pore pressure ratio,  $r_{u,r}$ ). The limiting  $\Delta u$  at the end of cyclic loading is estimated by the intersection of the static shear stress and the friction angle at "phase transformation" (Fig. 3). For the analyses herein, the phase transformation angle is taken as equal to the critical state friction angle ( $\phi'_{cv}$ ) for estimating the limiting  $r_{u,r}$  or  $\Delta u$ . The actual mobilized friction angle at the end of shaking could be slightly greater or smaller depending on the actual stress history and any partial drainage during shaking. Thus cyclic loading brings points A & C over to phase transformation without any change in void ratio, as shown in Figure 2.

Pore water flow after shaking then causes the sand at Point C to contract (densify) and the sand at Point A to dilate (loosen) (Figure 2). At both

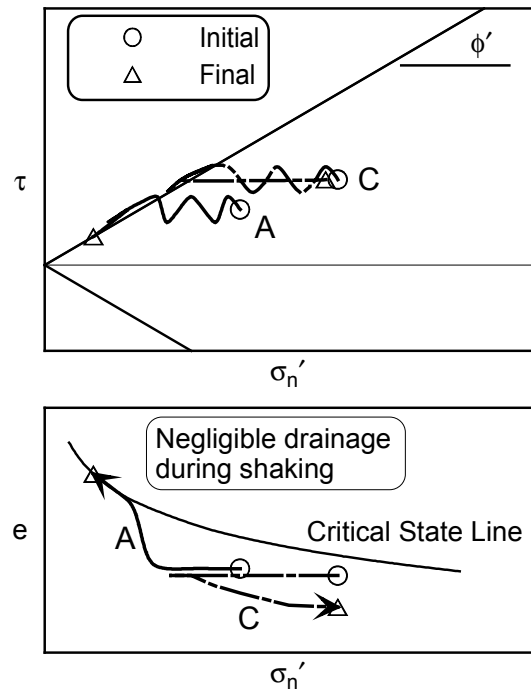


Figure 2: Possible stress path from start of cyclic loading to conclusion of void redistribution.

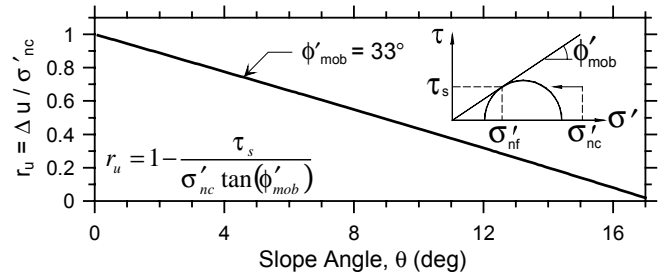


Figure 3: Limiting residual pore pressure ratio versus the slope angle of the infinite slope.

points, the sand carries a constant static shear stress that is imposed by the slope. At point C, the net outflow of water results in an increase in effective stress. At Point A, the net inflow of pore water causes the sand to progressively dilate (loosen) and shear at an approximately constant effective stress until it reaches critical state. After the sand at Point A reaches critical state, the further inflow of pore water will result in further loosening such that the sand's critical state shear strength is less than that required for stability of the slope, and thus the slope will fail along a localized shear zone at the top of the sand layer.

### 3 DETAILED EXAMPLE

An example is presented to illustrate specific features of the analysis method and void redistribution mechanism. Referring to the slope schematic in Figure 1, the top and bottom layers

are taken as 3-m thick ( $H_t = H_b = 3$  m) and their densities are taken as equal. The liquefiable layer consists of sand with a  $\phi'_{cv}$  of  $33^\circ$ , an initial  $D_r$  of 50%, and minimum and maximum dry densities of  $1.333 \text{ g/cm}^3$  and  $1.635 \text{ g/cm}^3$ . The slope angle  $\theta$  is  $10^\circ$ . As previously stated, the factor of safety against triggering of liquefaction (generation of limiting  $r_u$ ) is unity ( $FS_L = 1.0$ ), the confining layer is essentially impermeable, and the time factor for layer consolidation is such that seepage during shaking is negligible.

Results of the analysis are summarized in Figure 4. Static shear stresses parallel to the ground surface are computed using infinite slope theory, and these static shear stresses remain constant as long as the slope is stable (Fig 4.a). The effective normal stress (on planes parallel to the ground surface) and pore water pressure at the end of shaking are determined using  $r_{u,r}$  calculated for  $\phi'_{mob} = \phi'_{cv}$  at the end of shaking (Fig. 4.b & 4.c). This condition results in a hydraulic gradient towards the ground surface (Fig. 4.d).

Point A at the top of the layer then experiences a net inflow of water as consolidation progresses after the end of shaking. The sand at point A dilates (loosens) and experiences a slight increase in excess pore pressure to a post-cyclic maximum value,  $u_{pc,max}$ , corresponding to the mobilization of the peak friction angle,  $\phi'_p$ . The sand is able to mobilize a greater friction angle during this inflow because it is dilating, as demonstrated by specialized triaxial tests that mimic this loading path (Boulanger & Truman 1996); This difference in mobilized friction angles is similar to that for

conventional drained versus undrained loading (Kutter & Chen 1997). The value of  $\phi'_p$  was calculated as  $38.6^\circ$  using Bolton's (1986) relations for estimating the peak dilation angle of a soil based on its  $D_r$  and confining stress.

The continued flow of water into point A will cause additional dilation (loosening) toward its critical state and a progressive drop in  $\phi'_{mob}$  from  $\phi'_p$  to  $\phi'_{cv}$ . At critical state, the shear strength of the soil if loaded undrained would be equal to the  $\tau_s$  acting parallel to the ground surface. Any additional flow into point A would cause instability because the critical state shear strength would drop below the applied shear stress.

A useful reference condition is a hydrostatic pore pressure distribution anchored at point A with  $u_{pc,max}$  (Fig. 4.d). The sand at point A will have developed its maximum dilation angle (and thus is at  $\phi'_p$ ) and a corresponding minimum effective stress (while still stable). This condition, as discussed below, defines the zone of sand at the top of the layer that will dilate (loosen) as pore water flows upward from the lower contracting (densifying) zones. Further inflow of pore water will cause the  $\phi'_{mob}$  to progressively decrease toward  $\phi'_{cv}$ , which progressively decreases the thickness of the dilating zone and leads to a thin localization at the top of the layer. The transition from  $\phi'_p$  to  $\phi'_{cv}$  is an unstable process (like strain softening) and hence the condition defined by having point A at  $\phi'_p$  represents the limit to the final distribution of  $u$  that will avoid the onset of this unstable localization process.

This reference condition defines the maximum

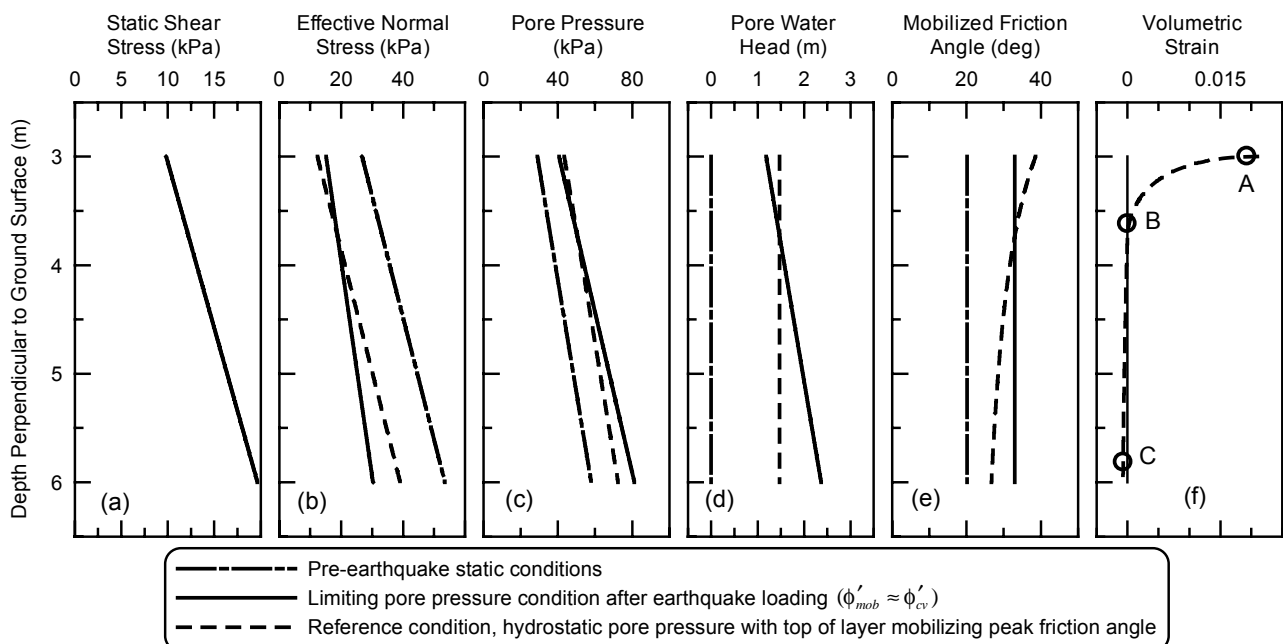


Figure 4: Void redistribution in confined sand layer ( $D_r = 50\%$ ) for an infinite slope with  $\theta = 10^\circ$ .

thickness of the dilation zone,  $h_{dil}$ , by identifying the point where the reference line crosses the limiting condition after shaking (Figs. 4.b-4.e). This intersection corresponds to the constant volume point B in Figures 1 and 4. All points above B dilate (loosen) and below B contract (densify). For this example, the  $h_{dil}$  is 0.73 m.

The next steps are to evaluate the volume of water that can be safely absorbed by the dilating (loosening) zone, which we call the "dilation capacity",  $V_{dil}$ , and compare it with the water produced by the contracting (densifying) zone,  $V_{con}$ . Note that when  $V_{con} > V_{dil}$ , there is a strong potential for localization at point A.  $V_{dil}$  is estimated by integrating the volumetric strain,  $\epsilon_v$ , between points A and B as  $u$  rises from  $u_{l,r}$  to the reference condition.  $V_{dil}$  is evaluated numerically using a  $\epsilon_v$ -versus- $\phi'_{mob}$  relation derived from the lab data by Boulanger and Truman (1996). The effect of  $D_r$  on this relation was then estimated using both the relative dilatancy index by Bolton (1986) and the relative state parameter index by Boulanger (2003).  $V_{con}$  is estimated by integrating  $\epsilon_v$  between points B and C as  $u$  drops from  $u_{l,r}$  to the reference condition.  $V_{con}$  is evaluated numerically using  $\Delta\epsilon = \lambda \ln(\Delta\sigma'_{ref}/\Delta\sigma'_1)$  with  $\lambda$  taken as 0.0053 for a  $D_r$  of 50%. The  $\epsilon_v$  variation versus depth is shown in Figure 4.f, from which  $V_{dil} = 0.0029 \text{ m}^3/\text{m}^2$  and  $V_{con} = 0.0010 \text{ m}^3/\text{m}^2$ . Since  $V_{dil} > V_{con}$ , the slope is expected to remain stable despite the fact that void redistribution caused the sand at point A to volumetrically expand by 1.9% (reducing its  $D_r$  from 50% to about 41%).

However, if the thickness of the liquefied sand layer,  $H_b$ , is greater than 5.1 m, then  $V_{con}$  becomes greater than  $V_{dil}$  and the slope would be considered potentially unstable by void redistribution. This  $H_b$  is the limiting thickness required for stability,  $H_{b,l}$  for  $FS_L = 1.0$ .

Instability with  $V_{con} > V_{dil}$  leads to a thin localization at point A that conceptually may only be mm's thick (i.e., 10's of  $D_{50}$ ). However, the thickness of this localization is much smaller than the thickness of sand that dilates during the initial

stages of upward seepage ( $h_{dil} = 0.73 \text{ m}$  in this example). If  $h_{dil}$  was a priori assumed to be only mm's thick, then  $V_{dil}$  and the limiting thickness required for stability,  $H_{b,l}$ , would be grossly underestimated. For example, if  $h_{dil} \approx 5 \text{ mm}$ , then  $H_{b,l}$  would only be 12 mm instead of the 5.1 m previously calculated.

#### 4 PARAMETRIC STUDY

The preceding analysis was repeated for  $\theta$  from  $0^\circ$  to  $16.5^\circ$  at  $D_r$  of 30%, 50%, and 70% to illustrate the effect of these parameters on the void redistribution mechanism. The sand's  $\lambda$  was taken as 0.0087, 0.0053, and 0.0030 for  $D_r$  of 30%, 50%, and 70%, respectively.

The thickness of the dilating zone,  $h_{dil}$ , increases with increasing  $D_r$  and increasing slope angle as shown in Figure 5, but is independent of the sand layer thickness  $H_b$ . These results illustrate how  $h_{dil}$  varies significantly and is generally much greater than 10's of  $D_{50}$ . At  $\theta = 16.5^\circ$ , the results for all three  $D_r$  indicate that  $h_{dil} = H_b$  (i.e., there is no contracting zone) because the upward hydraulic gradient is zero after shaking. However, this surprising result coincides with the factor of safety against static slope instability being equal to unity at  $\theta = 16.5^\circ$  (since  $\phi'_{cv} = 33^\circ$  and the water table is at ground surface).

The variation of  $V_{con}$  and  $V_{dil}$  with  $D_r$  and slope angle is shown in the lower portion of Figure 6 for the case where  $H_t$  and  $H_b$  are both 3 m. A steeper slope and greater  $D_r$  increase the dilation capacity ( $V_{dil}$ ) and reduce the volume of water expelled from the contracting zone ( $V_{con}$ ). The intersection of the  $V_{dil}$  and  $V_{con}$  curves for the same  $D_r$  represents the  $\theta$  that divides stable versus unstable conditions for this particular model. The upper portion of Figure 6 compares the ratio  $V_{dil}/V_{con}$ , which is  $> 1$  for stable conditions, to the static factor of safety of the slope,  $FS_{static}$ . This shows that while a steeper slope will be less likely to develop localization due to void redistribution, the overall static stability of the slope is lower.

The influence of liquefied layer thickness is illustrated in Figure 7 by plotting the limiting thickness required for stability,  $H_{b,l}$ , versus  $D_r$  for  $\theta = 4^\circ, 8^\circ, \text{ and } 12^\circ$ . Sand layers thinner than  $H_{b,l}$  would be expected to remain stable, whereas thicker layers could become unstable (i.e.,  $H_{b,l}$  corresponds to  $V_{dil} = V_{con}$ ). The value of  $H_{b,l}$  increases with increasing  $D_r$  or  $\theta$ . For example, the curve for  $\theta = 8^\circ$  shows that a  $D_r = 30\%$  sand layer would be unstable if it was thicker than 1.0 m while a  $D_r = 70\%$  sand layer would only be unstable if it was thicker than about 6.4 m.

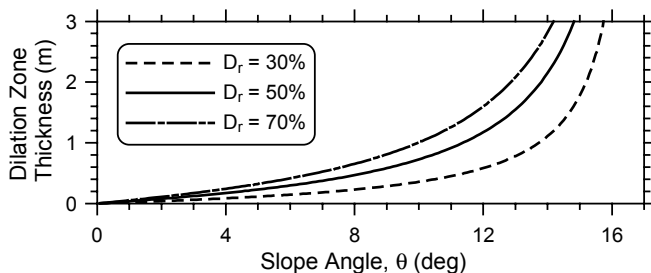


Figure 5: Dilating zone thickness versus  $\theta$ .

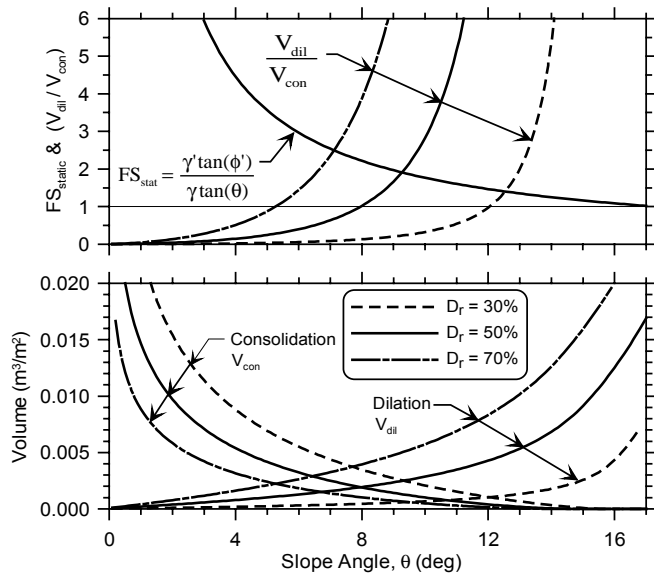


Figure 6: Ratio of dilation capacity to volume generated, compared to the static factor of safety. ( $FS_L = 1.0$ )

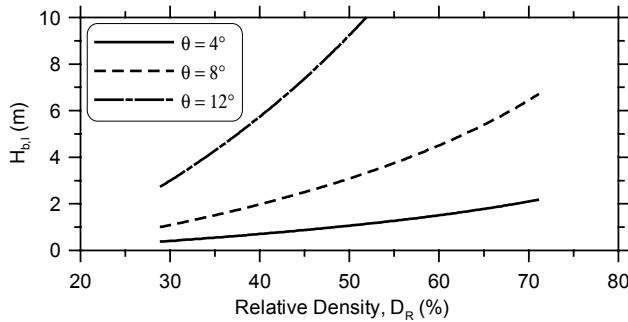


Figure 7: Limiting thickness of base layer that leads to void redistribution-induced localization. ( $FS_L = 1.0$ )

## 5 DISCUSSION

The analysis results summarized in Figures 5-7 indicate that  $H_{b,l}$  theoretically approaches zero as  $\theta$  approaches zero regardless of  $D_r$ , but in reality there are practical considerations that would limit  $H_{b,l}$  to some finite nonzero thickness. For  $\theta = 0$ , the absence of static shear stresses parallel to the ground surface means that there is no dilating zone ( $h_{dil}=0$ ) and hence any nonzero liquefied layer thickness would theoretically produce a water film at the top according to the idealized boundary conditions imposed by the analysis. In reality, water from the liquefied sand can be expected to seep into the overlying layer, whether by advection of flow into cracks or pipes that form in the overlying soil. For a thin liquefied sand layer, this outward flow could either preclude

water film formation or collapse a water film that temporarily forms. The resulting ground deformations (settlements, lateral spreading) depend on numerous additional factors, but it is intuitive that in many cases the sand layer would have to be thicker than some minimum value before any surface deformations were noticeable.

Roughness or irregularity of the interface between the liquefied sand layer and the overlying soil (i.e., potential sliding plane) can be expected to affect both the thickness of the dilating zone and the consequences of water film formation. For sloping ground conditions, it is possible that temporary arching of shear stresses between irregularities could result in localized pockets where the shear stress drops to zero and a water film can more easily form. Subsequent ground movements and cracking could redistribute shear stresses, collapse or relieve existing water films (e.g., by piping up into ground cracks), and lead to water film formation in other localized zones.

The intensity and duration of shaking was assumed to be just sufficient to increase the pore pressures to their limiting value in the above analyses, regardless of the soil's  $D_r$ . Thus, for a given level of shaking, the role of  $D_r$  will generally be greater than indicated in Figures 5-7 because a greater  $D_r$  means greater resistance to the generation of excess pore water pressure.

Kulasingam (2002) analyzed the timing of void redistribution within a similarly idealized infinite slope using finite difference and dimensional analysis methods. The results of those analyses showed how the volume of water expelled from the lower contracting zone ( $V_{con}$ ) was affected by the duration of shaking, the intensity of shaking, the permeability and compressibility of the sand, and other factors. The fraction of void redistribution that occurs during versus after shaking was dependent on the same factors, plus the thickness and properties of the overlying soil layer. These effects are easily incorporated into the analysis method presented herein, but that is beyond the scope of this paper.

Seismic loading of sloping ground can cause reversal of shear stress directions, such that the soil temporarily goes through a state of zero shear stress. In that situation,  $r_u$  may temporarily equal 100% even though the post-earthquake limiting  $r_{u,r}$  will be less than 100% due the influence of the slope (Figure 3). The effects of cyclic fluctuations in  $r_u$  and shear stress during shaking are hard to assess but intuitively will depend on seepage rates relative to the duration of shaking, the roughness of the potential sliding plane, and other factors.

Increasing the slope angle may not affect two-

dimensional embankments the same way as infinite slopes. Consider a thin horizontal sand layer that extends from beneath the center of an embankment dam out to near its toe. If the sand layer is bounded by low permeability soils and is saturated, then the triggering of liquefaction will produce greater pore water pressures beneath the embankment center than at the toe. Pore water would then flow horizontally toward the toe region where dilation (loosening) may occur. The volume of the contracting (densifying) zone can thus be much greater than represented by the sand layer thickness alone.

## 6 CONCLUSIONS

Void redistribution in liquefied soil remains a poorly understood phenomenon that is difficult to quantitatively predict in practice for a myriad of complicating reasons, many of which were discussed above (e.g., heterogeneity of geologic deposits, formation of cracks and sand boils, and uncertainty of seismic shaking intensity). Nonetheless, an understanding of the basic mechanisms can lead to improved judgments regarding the potential severity of void redistribution in the field and the appropriate means for mitigating its effects.

An analysis of void redistribution in liquefied soil in a layered infinite slope was presented that illustrates key features of behavior and distinguishes between conditions that theoretically lead to localization. The condition for localization due to void redistribution is reached when the volume of water supplied to a dilating zone exceeds the dilation capacity. The potential for instability by this mechanism was shown to depend strongly on the sand's relative density ( $D_r$ ), the slope angle ( $\theta$ ), and the sand layer thickness ( $H_b$ ). The analysis method can be combined with other methods for describing pore pressure generation and dissipation, and thus account for the effects of shaking duration, shaking intensity, stratigraphy, and soil properties (permeability, compressibility, and cyclic loading resistance for each soil).

The initial thickness of the dilating (loosening) zone at the top of the sand layer is much greater than the final thickness of the localized shear zone (i.e., 10's of  $D_{50}$ ). This dilating zone can accommodate a certain volume of pore water inflow, which we call dilation capacity. Greater inflow will cause the dilating zone to decrease in thickness until shear localization does in fact occur. Not accounting for the initial thickness of this dilating zone results in an overly conservative

assessment of the conditions that lead to instability.

## 7 ACKNOWLEDGEMENTS

The National Science Foundation funded this research under grant CMS-0070111.

## 8 REFERENCES

- Bolton, M. D. (1986). The strength and dilatancy of sands. *Géotechnique*, 36(1), 65–78.
- Boulanger, R. W., & Seed, R. B. (1995). Liquefaction of sand under bi-directional monotonic and cyclic loading. *J. Geot. Eng.*, ASCE, 121(12), 870-878.
- Boulanger, R. W. & Truman, S. P. (1996). Void redistribution in sand under post-earthquake loading. *Canadian Geotechnical J.*, 33, 829–834.
- Boulanger, R. W. (1999). Void redistribution in sand following earthquake loading. *Physics and Mechanics of Soil Liquefaction*, Lade & Yamamuro, eds. Balkema, Rotterdam, 261–268.
- Boulanger, R. W. (2003). Relating  $K_\alpha$  to a relative state parameter index. *J. Geot. & Geoen. Eng.*, ASCE, in press.
- Dobry, R. & Liu, L. (1992). Centrifuge modeling of soil liquefaction, in *Proc. 10<sup>th</sup> World Conf. On Earthquake Engineering., Madrid, July 1992.* vol. 11, 6801–6809.
- Fiegel, G. L., & Kutter B. L. (1994). Liquefaction mechanism for layered soils. *J. Geot. Eng.*, ASCE, 120(4), pp 737-755.
- Kokusho, T. (1999). Water film in liquefied sand and its effect on lateral spread. *J. Geot. Geoen. Eng.*, ASCE, 125(10), 817 – 826.
- Kulasingam, R. (2003). *Effects of Void Redistribution on Liquefaction-Induced Deformations.* Ph.D. thesis, Univ. Calif., Davis.
- Kutter, B. L. & Chen, Y. R. (1997). Constant  $p'$  and Constant volume friction angles are different. in, *ASTM Geot. Testing J.*, GTJODJ, 20(3), pp 304 – 316.
- Liu, H. & Qiao, T. (1984). Liquefaction potential of saturated sand deposits underlying foundation of structure. *Proc. 8<sup>th</sup> World Conf. Earthquake Engrg*, San Francisco, Vol. 3, 199–206.
- Malvick, E. J., Kulasingam, R., Kutter, B. L. & Boulanger, R. W. (2002). Void redistribution and localized shear strains in slopes during liquefaction. *Physical Modelling in Geotechnics, ICPMG 02*, R. Phillips, P. Guo, R. Popescu, eds., A. A. Balkema, 495-500.
- National Research Council [NRC] (1985). *Liquefaction of Soils During Earthquakes.* National Academy Press, Washington, D.C.
- Tokimatsu, K., Tata, Y., & Zhang, J. M. (2001). Effects of pore water redistribution on post-liquefaction deformation of sands, in *Proc. 15<sup>th</sup> Intl. Conf. Soil Mech. Geotech. Engrg.*, Istanbul, Turkey, Vol. 1, 289–292.
- Vaid, Y. P., and Eliadorani, A. (1998). Instability and liquefaction of granular soils under undrained and partially drained states. *Can. Geot. J.*, 35, pp 1053 - 1062.
- Whitman, R. V. (1985). On liquefaction, in *Proc. 11<sup>th</sup> Intl. Conf. Soil Mech. Fndtn. Engrg.* San Francisco, CA. vol. 11, 1923–1926